

42. V. C. Gulick, M. S. Marley, V. R. Baker, *Lunar Planet. Sci.* **XXII**, 509 (1992).
43. H. E. Newsom, *Icarus* **44**, 207 (1980); G. R. Brakenridge, H. E. Newsom, V. R. Baker, *Geology* **13**, 859 (1985).
44. J. M. Goldspiel, thesis, Cornell University, Ithaca, NY (1994).
45. In this model, the heat diffusion equation is solved for a porous regolith, with terms for advection by moving fluid and treatment of freezing or melting within pores. The equations of fluid flow are solved for spatially and temporally variable hydraulic conductivity, with variations caused by

- pore freezing or melting. The outer thermal boundary condition takes into account radiation and conduction at the seepage face, both to and from the atmosphere, and the effects of wind.
46. M. H. Carr, *J. Geophys. Res.* **84**, 2995 (1979).
47. W. H. Brutsaert, *Evaporation Into the Atmosphere: Theory, History, and Applications* (Reidel, Boston, 1982).
48. This gradient is determined from Earth-based radar altimetry of regional slopes in ancient martian drainage basins [J. M. Goldspiel, S. W. Squyres, M. A. Slade, R. F. Jurgens, S. H. Zisk, *Icarus* **106**, 346 (1993)] and hence probably

- overestimates actual channel gradients.
49. D. Wallace and C. Sagan, *ibid.* **39**, 385 (1979); M. H. Carr, *ibid.* **56**, 476 (1983).
50. V. R. Baker, M. H. Carr, V. C. Gulick, C. R. Williams, M. S. Marley, in (23), pp. 493-522.
51. C. E. Sloan, C. Zenone, I. R. Mayo, *U.S. Geol. Surv. Prof. Pap.* **979** (1976).
52. J. A. Baross and S. E. Hoffman, *Origins Life* **15**, 327 (1985).
53. This work was supported by the National Aeronautics and Space Administration Planetary Geosciences and Martian Surface and Atmosphere Through Time programs.

## RESEARCH ARTICLE

# Volume Holographic Storage and Retrieval of Digital Data

John F. Heanue, Matthew C. Bashaw, Lambertus Hesselink\*

A multiple page fully digital holographic data storage system is demonstrated. This system is used to store and retrieve digital image and compressed video data with a photorefractive crystal. Architecture issues related to spatio-rotational multiplexing and novel error-correcting encoding techniques used to achieve low bit-error rates are discussed.

Holographic storage has long held promise for large digital storage capacity, fast data transfer rates, and short access times (1, 2). Current storage technologies are limited in that they do not simultaneously provide each of these three features. Recent developments in materials, spatial light modulators (SLMs), and charge-coupled-device (CCD) arrays have brought the promise closer to reality. Potential storage capacity of terabytes of data, transfer rates exceeding 1 gigabit per second, and random access times less than 100  $\mu\text{sec}$  appear feasible, making holographic storage attractive for applications in the planned national information infrastructure, in conventional and parallel computing, and in the entertainment industry.

Holographic recording is accomplished by combining an image-bearing light beam and a reference beam in a recording medium. The variation in intensity in the resulting interference pattern causes the complex index of refraction to be modulated throughout the volume of the medium. In a photorefractive medium such as  $\text{LiNbO}_3$ , charges are excited from impurity centers in the presence of light and subsequently trapped (3, 4). The resulting space-charge field causes modulation in the index of refraction through the electro-

optic effect. When the medium is exposed to a reference beam identical to one used in recording, the light will diffract in such a way as to reproduce the original image-bearing wavefront. In holographic data storage, data are converted to an optical signal by use of an SLM (Fig. 1). A hologram corresponding to the image (one data "page") on the SLM is then recorded in a photorefractive crystal or other suitable volume holographic recording medium. Multiple holograms, each corresponding to a page of data, are written in the medium using angular multiplexing, in which each hologram is written with a reference beam incident at a different angle. For a 1-cm-long  $\text{LiNbO}_3$  crystal, holograms may be written with reference beams separated in angle by as little as 50  $\mu\text{rad}$ . The angle can be changed either by steering the beam or by rotational multiplexing, a technique that in-

volves mechanical rotation of the storage medium. The collection of stored data pages superimposed in a particular volume of the crystal is referred to as a stack. Spatial multiplexing is accomplished by dividing the crystal volume into a number of regions and recording one stack per region. Readout of a stored data page involves illuminating the crystal with the appropriate reference beam and imaging the diffracted optical signal onto a CCD array, which converts the optical signal back into an electronic signal. With parallel readout of the CCD array, fast data transfer rates can be achieved because all pixels in the stored data page are reconstructed simultaneously.

**Performance criteria.** The main criteria used in evaluating the performance of a holographic data storage system are capacity, data transfer rate, access time, and bit error rate. The transfer rate and access time are bounded by the speed of peripheral devices (electronic beam steerers, mechanical stages, CCD array), whereas capacity and bit error rate are determined by the noise level in the system. As the number  $N$  of holograms stored in a single stack increases, the diffraction efficiency falls as  $1/N^2$ . As the strength of the diffracted signal decreases, the signal-to-noise ratio (SNR) decreases because the strength of noise due to scatter is independent of  $N$ . The total number of holograms that can be stored is thus determined by the minimum acceptable SNR. A lower bound on the bit error rate (BER) can be determined using the SNR calculated assuming a  $1/N^2$  falloff in diffraction efficiency; in practice, the

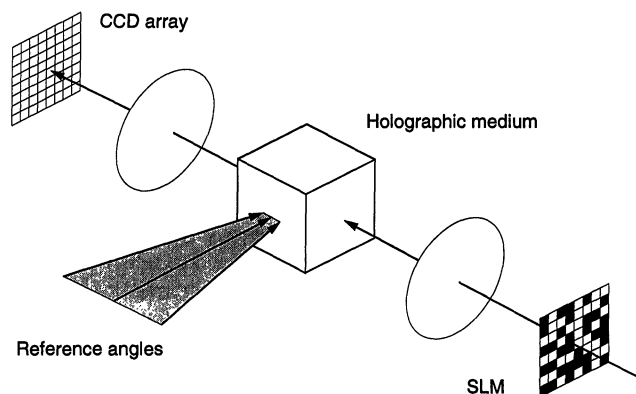
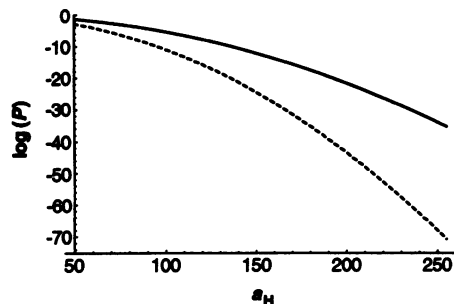
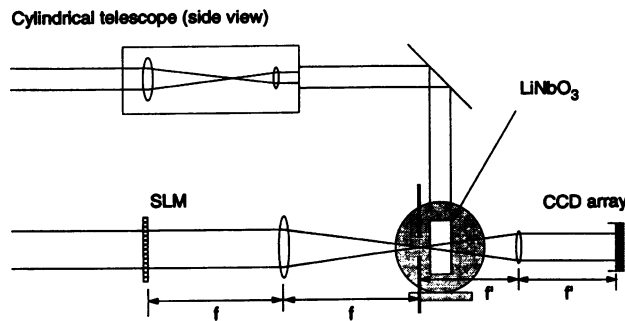


Fig. 1. General holographic recording scheme.

J. F. Heanue is in the Department of Applied Physics, Stanford University, Stanford, CA 94305-4090, USA. M. C. Bashaw and L. Hesselink are in the Department of Electrical Engineering, Stanford University, Stanford, CA 94305-4035, USA.

\*To whom correspondence should be addressed.

**Fig. 2.** Top view of the holographic data storage system. Entrance and exit optics have focal lengths  $f$  and  $f'$ , respectively.



**Fig. 3.** The logarithm of the probability of error versus mean detected ON amplitude when a 0 is transmitted for threshold detection (solid line) and differential detection (dashed line).

BER is further limited by page-to-page and intrapage fluctuations in signal strength. These noise sources limit the effectiveness of volume holography for the direct storage of images in analog form.

The noise-tolerant nature of digital storage makes it possible to overcome problems associated with the aforementioned noise sources; however, to the best of our knowledge, no fully automated digital holographic data storage system has been implemented and no comprehensive study of the BER performance of a system operating at reasonable data transfer rates has been carried out. The majority of previous holographic storage implementations have involved direct storage and retrieval of pictorial information. For example, Mok has demonstrated angular-multiplexed storage of as many as 5000 edge-enhanced analog images in a single crystal (5). The achievable BER has been projected by sampling a small number of digital information bits from a random sampling of 1000 holograms stored in a manually Bragg-tuned system (6). Using various encoding techniques, we have implemented a fully automated system in which data are written and recalled in digital form. Although any type of digital data can be stored, we have used our spatio-rotational multiplexing system to store digital representations of color images and compressed video. Critical features of our implementation include location of the Fourier plane outside the crystal volume,

use of cylindrical lenses to implement spatial multiplexing, use of a differential encoding technique to increase error immunity, use of Hamming error correction codes, and the distribution of consecutive information bits over multiple data pages in order to decrease the probability of burst errors. With these techniques, a BER of  $10^{-6}$  has been achieved at readout rates of  $6.3 \times 10^6$  pixels per second with a total capacity of 163 kilobytes (kB). Access times were limited by the use of mechanical stages and no permanent fixing of the stored data was implemented. We have used the system to evaluate tradeoffs between BER and storage capacity at a fixed data transfer rate.

**The data storage system.** The storage medium in our system (Fig. 2) is an Fe-doped  $\text{LiNbO}_3$  crystal cut such that its  $c$  axis is at 45 degrees to the crystal surfaces. The crystal dimensions are  $2 \text{ cm} \times 1 \text{ cm} \times 1 \text{ cm}$ , of which only a  $0.1\text{-cm}^3$  portion is used for data storage. The crystal is mounted on a computer-controlled rotation stage, which is in turn mounted on a computer-controlled translation stage, allowing the crystal to be moved in the vertical direction (perpendicular to the plane of the page in Fig. 2). The SLM is a  $480 \times 440$  pixel liquid crystal array taken from an InFocus TVT-6000 video projector. It is addressed with an analog video signal produced by a framegrabber board in the computer. The camera is an intensified CCD array. Each stored hologram is read out in 1/30 second. The cylindrical lenses in the reference beam path are used to collimate the reference to an area of approximately  $10 \text{ mm} \times 2 \text{ mm}$  at the face of the crystal. The combination of the translation stage and the collimation of the reference beam allows holograms to be stored in 4 different stacks. The signal beam occupies an area of approximately  $1.5 \text{ mm} \times 1.5 \text{ mm}$  on the front face of the crystal. The Fourier plane is located approximately 3 mm in front of the crystal. A filter is used to select only the central spot of the Fourier transform. The filter prevents erasure of previously recorded stacks during writing and eases alignment tolerances at the CCD plane. By locating the Fourier plane outside the crystal, re-

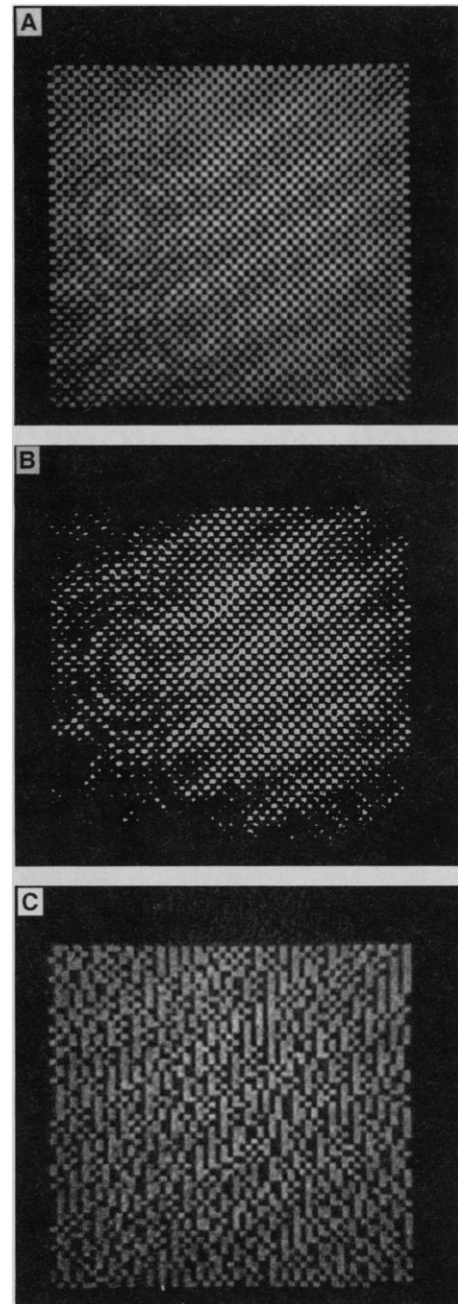


**Fig. 4.** (A) Reconstruction of an image stored in the crystal, (B) threshold version of the same image, and (C) differential encoded data page.

coding occurs in a Fresnel region, where the modulation depth is sufficiently uniform to eliminate the need for a diffuser (7).

Because previously recorded holograms are erased as additional holograms are recorded, an appropriate recording schedule must be determined in order to store a large number of pages. For symmetric write and erase times, equal diffraction efficiencies for each recorded hologram result from using recording times given by (8)

$$t_n = \tau \ln \left( \frac{1 + (n-1)\beta}{1 + (n-2)\beta} \right) \quad (1)$$

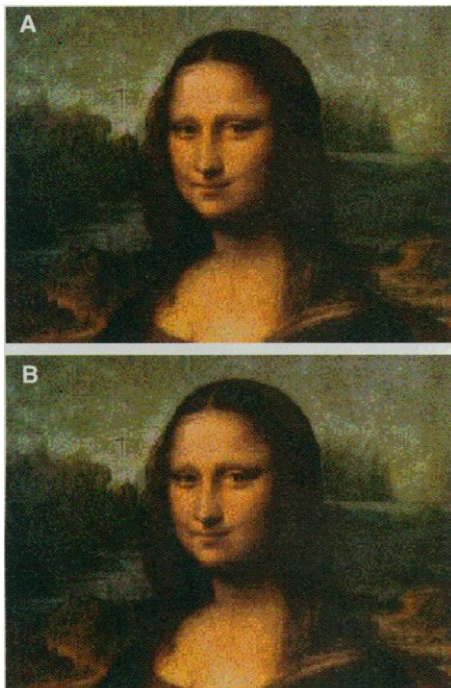


**Fig. 5.** (A) Picture displayed from the original data file and (B) picture displayed from a file copied from the holographic data storage system.

where  $t_n$  is the recording time of the  $n$ th hologram,  $\tau$  is the photorefractive time constant, and  $\beta$  is the ratio of the index of refraction modulation recorded during the first exposure to the saturation index modulation. For unequal time constants, numerical methods can be used to calculate appropriate recording times (9).

If all holograms result in equal diffraction efficiencies and each page is uniformly reconstructed, a threshold intensity can be chosen to distinguish ON pixels from OFF pixels. Note that we use “OFF” and “ON” when referring to SLM or CCD pixels and “0” and “1” when referring to information bits. An incorrect measurement of the time constant results in a schedule which leads to unequal diffraction efficiencies for each of the stored holograms. A 10 percent error in the assumed time constant can cause more than a factor of 2 variation in diffraction efficiency. In addition, laser fluctuations or anomalous writing behavior can contribute to diffraction efficiency variation. Intrapage distortion can arise from poor overlap of signal and reference beams in the crystal, nonuniform illumination of the SLM, introduction of interference fringes due to multiple reflections in the optical system, or nonuniformity of the SLM or CCD array.

**Differential encoding.** Page-to-page and intrapage signal variation severely limits the attainable BER in a system based on threshold detection. In order to circumvent

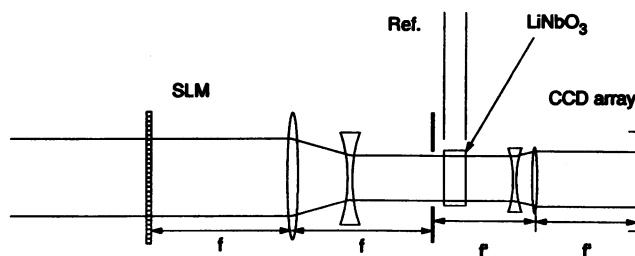


**Fig. 6.** Anamorphic imaging system used to access the entire crystal volume.

this problem, we use a differential encoding technique, in which the pixel sequence OFF-ON is written to the SLM to represent a 0 and the pixel sequence ON-OFF is written to represent a 1. At the detector, the sign of the difference in the intensity of adjacent pixels is used to determine the value of the detected information bit. In addition to being insensitive to page-to-page intensity fluctuations, the differential encoding technique results in a lower probability of error assuming a model of additive white noise which is independent from pixel to pixel. For example, the probability of an error given that a 0 is transmitted in a threshold detection system is given by (10, 11)

$$p \approx \int_{a_T}^{\infty} \frac{r}{\sigma^2} \exp\left(-\frac{r^2 + a_L^2}{2\sigma^2}\right) I_0\left(\frac{ra_L}{\sigma^2}\right) dr \quad (2)$$

where the threshold  $a_T$  is equal to  $(a_H + a_L)/2$ ,  $a_H$  and  $a_L$  are the average amplitudes of ON and OFF pixels, respectively, at the CCD array,  $\sigma$  is the standard deviation of the noise, and  $I_0$  is the zero order modified Bessel function of the first kind. The probability of an error given that a 0 is transmitted in a differential detection system is given by

$$p \approx \int_0^{\infty} \frac{x}{\sigma^2} \exp\left(-\frac{x^2 + a_L^2}{2\sigma^2}\right) I_0\left(\frac{xa_L}{\sigma^2}\right) dx \int_0^{\infty} \frac{r}{\sigma^2} \exp\left(-\frac{r^2 + a_H^2}{2\sigma^2}\right) I_0\left(\frac{ra_H}{\sigma^2}\right) dx dr \quad (3)$$

The advantage of differential encoding is clearly seen in Fig. 3, which shows plots of the logarithm of the above probabilities as a function of  $a_H$  for  $a_L = 0$  and  $\sigma = 10$ . When a substantial contribution to the variance is due to large-scale intrapage nonuniformities, we expect differential encoding to offer further improvement over thresholding than that shown in Fig. 3. Figure 4A shows a data page transmitted through the crystal and Fig. 4B shows a threshold version of the same image. Note that errors caused by interference fringes are evident even in the threshold image. Clearly, uniform threshold detection will not work in this case (although the system may be calibrated by passing a uniform image through and assigning a threshold level to

each pixel, assuming that errors are stationary in time). Figure 4C shows a differential encoded data page.

Ideally, each pixel on the SLM would be used to represent a single bit of data. The liquid crystal array used in our experiments exhibits some interpixel crosstalk. Pixels adjacent to an ON (transmitting) pixel exhibit a significant amount of transmission. Also, the SLM and the CCD array are manufactured with different horizontal to vertical pixel pitch ratios. Thus, with a simple optical system such as ours, it is impossible to image the SLM onto the CCD array such that each SLM pixel is imaged directly onto a CCD pixel. In practice, a multiple lens arrangement could be used to achieve the proper anamorphic imaging; however, this greatly increases system complexity. The pitch mismatch results in a systematic geometrical source of errors if too fine a sampling grid is used. In order to circumvent these problems, we use a block of  $8 \times 8$  pixels to represent one bit. The differential encoding technique increases the pixel-to-bit ratio to  $8 \times 16$  pixels per information bit. The data are read out by sampling the CCD output at one pixel for each  $8 \times 8$  pixel block imaged onto it. The difference in intensity between adjacent samples is used to determine whether the information bit is a 0 or a 1.

**Performance characteristics.** We measured the raw BER of our system to be between  $10^{-3}$  and  $10^{-4}$  at video readout rates. In order to improve performance, we implemented a Hamming error correcting code (12) in which four check bits are added to each string of eight data bits. The Hamming code is capable of correcting a single bit error in the sequence of 12 bits assuming that only one bit error occurs in those 12. In order to reduce the potential of burst errors, each stored data page represented one bit plane in a two-byte sequence. Thus, each bit in the 12-bit sequences was stored in a separate page in order to reduce the probability of multiple errors within a given sequence. With the error-correcting codes, we were able to achieve a BER of  $10^{-6}$ , which is adequate for compressed video storage and more than sufficient for uncompressed image storage. We used our system to store both digital color image and video data. Figure 5 shows

an example of a displayed data file and the same file after being transferred to and read back from the holographic data storage system. The total capacity of the system is four 308-page stacks with 1592 bits per page, resulting in a raw capacity of 245 kB. Taking into account the necessary error-correcting bits, the total useful data capacity is 163 kB. The total pixel capacity of our system is  $2.6 \times 10^8$  pixels, with a density of  $3 \times 10^9$  pixels per cubic centimeter. The transfer rate is  $6.3 \times 10^6$  pixels per second. The CCD camera outputs one byte per pixel. The total pixel capacity of our system indicates that our storage capacity does not represent a fundamental limit. Rather, the primary limitation in determining the information storage capacity is the necessary oversampling on the SLM. With a higher quality SLM designed in conjunction with the CCD array, we anticipate that the information capacity and data transfer rates can be enhanced by several orders of magnitude.

Our current system does not fully utilize the available crystal volume. Capacity can be increased by using an anamorphic imaging system (Fig. 6) in the signal beam path. The system focuses the signal beam to an area of approximately  $1.5 \text{ mm} \times 20 \text{ mm}$ , so that nearly the entire crystal volume is used in the four stacks. An anamorphic imaging arrangement can cause the system to become more sensitive

to nonuniformities in the crystal. The increase in susceptibility to errors while increasing capacity represents a fundamental tradeoff meriting further investigation.

Our implementation represents an investigation of the performance of a digital holographic storage system, but additional improvements are needed before a useful commercial device can be produced. In applications such as read-only memory (ROM), a fixing process can be used to ensure long-term storage of the data, which will otherwise gradually erase during repeated read operations. In our experiments, no fixing was attempted; however, thermal techniques have previously been shown to provide long-term erasure-resistant image storage in  $\text{LiNbO}_3$  (13–15). In addition, systems techniques can be used in some applications to preserve the fidelity of stored images (16–18). It is also desirable in a practical device to implement angular multiplexing with electro-optic or acousto-optic beam steerers rather than mechanical stages. Implementation without moving parts provides increased reliability as well as potentially faster access times. The total storage capacity and system performance might be greatly enhanced with improvements in SLM, CCD, and materials technology as well as improvements to the optical system. It is anticipated that improved components and materials will be available in the next few years through

research in other consumer electronics and computer applications areas.

## REFERENCES AND NOTES

1. P. J. van Heerden, *Appl. Opt.* **2**, 393 (1963).
2. L. Hesselink and M. C. Bashaw, *Opt. Quant. Electron.* **25**, S611 (1993).
3. F. S. Chen, J. T. LaMacchia, D. B. Frazer, *Appl. Phys. Lett.* **13**, 223 (1968).
4. D. L. Staebler, W. J. Burke, W. Phillips, J. J. Amodel, *ibid.* **26**, 182 (1975).
5. F. H. Mok, *Opt. Lett.* **18**, 915 (1993).
6. F. Mok, D. Psaltis, G. Burr, *Proc. Soc. Photo-Opt. Instrum. Eng.* **1773**, 334 (1992).
7. R. Brauer, U. Wojak, F. Wyrowski, O. Bryngdahl, *Opt. Lett.* **16**, 1427 (1991).
8. E. S. Maniloff and K. M. Johnson, *J. Appl. Phys.* **70**, 4702 (1991).
9. F. H. Mok, M. C. Tackitt, H. M. Stoll, *Opt. Lett.* **16**, 605 (1991).
10. W. Lee, *J. Opt. Soc. Am.* **62**, 797 (1972).
11. J. W. Goodman, *Statistical Optics* (Wiley, New York, 1985).
12. R. W. Hamming, *Coding and Information Theory* (Prentice-Hall, Englewood Cliffs, NJ, 1986).
13. J. J. Amodel and D. L. Staebler, *Appl. Phys. Lett.* **18**, 540 (1971).
14. H. Kurz, *Philips Tech. Rev.* **37**, 109 (1977).
15. V. I. Bobrinev, Z. G. Vasil'eva, E. Kh. Gulanyan, A. L. Mikaelyan, *Zh. Eksp. Teor. Fiz. Pis'ma Red.* **18**, 267 (1973).
16. S. Boj, G. Pauliat, G. Roosen, *Opt. Lett.* **17**, 438 (1992).
17. H. Sasaki, Y. Fainman, J. E. Ford, Y. Taketomi, S. H. Lee, *ibid.* **16**, 1874 (1991).
18. D. Brady, K. Hsu, D. Psaltis, *ibid.* **15**, 817 (1990).
19. This research has been financially supported in part by the Advanced Research Projects Agency through contract number N00014-92-J-1903.

4 May 1994; accepted 15 June 1994

## AAAS–Newcomb Cleveland Prize

### To Be Awarded for a Report, Research Article, or an Article Published in *Science*

The AAAS–Newcomb Cleveland Prize is awarded to the author of an outstanding paper published in *Science*. The value of the prize is \$5000; the winner also receives a bronze medal. The current competition period began with the 3 June 1994 issue and ends with the issue of 26 May 1995.

Reports, Research Articles, and Articles that include original research data, theories, or syntheses and are fundamental contributions to basic knowledge or technical achievements of far-reaching consequence are eligible for consideration for the prize. The paper must be a first-time publication of the author's own work. Reference to pertinent earlier work by the author may be included to give perspective.

Throughout the competition period, readers are invited to nominate papers appearing in the Reports, Research Articles, or Articles sections. Nominations must be typed, and the following information provided: the title of the paper, issue in which it was published, author's name, and a brief statement of justification for nomination. Nominations should be submitted to the AAAS–Newcomb Cleveland Prize, AAAS, Room 924, 1333 H Street, NW, Washington, DC 20005, and **must be received on or before 30 June 1995**. Final selection will rest with a panel of distinguished scientists appointed by the editor-in-chief of *Science*.

The award will be presented at the 1996 AAAS annual meeting. In cases of multiple authorship, the prize will be divided equally between or among the authors.